ELSEVIER

Noise-induced basin hopping in a vibro-impact system

Silvio L.T. de Souza [a], Antonio M. Batista [b], Iberê L. Caldas [a],
Ricardo L. Viana [c,*], Tomasz Kapitaniak [d]

[a] *Instituto de Física, Universidade de São Paulo, C.P. 66318, 05315-970 São Paulo, São Paulo, Brazil*
[b] *Departamento de Matemática e Estatística, Universidade Estadual de Ponta Grossa, 84030-900, Ponta Grossa, Paraná, Brazil*
[c] *Departamento de Física, Universidade Federal do Paraná, C.P. 18081, 81531-990 Curitiba, Paraná, Brazil*
[d] *Division of Dynamics, Technical University of Lódz, Stefanowskiego 1/15, 90-924 Lódz, Poland*

Abstract

The dynamics of vibro-impact systems of engineering interest is numerically studied by means of a prototype consisting of an oscillating cart containing a ball undergoing inelastic collisions with its walls. We have described a multistable regime, for which different attractors coexist with a complicated basin boundary structure in the phase space. We investigated the effect of adding a certain amount of parametric noise in this model, focusing on the basin hopping, i.e., the intermittent switching between basins of different attractors.
© 2005 Elsevier Ltd. All rights reserved.

1. Introduction

Vibro-impact oscillators have moving parts colliding with either moving or stationary components, and are often found in engineering applications, as vibration hammers, driving machinery, milling, impact print hammers, and shock absorbers [1,2]. The practical interest in the study of vibro-impact oscillators lies in both their desirable and undesirable effects. The former are the basis of their operation, like an impact hammer, whereas the latter can be exemplified by large amplitude response leading to material fatigue and rattling in gearboxes, bearings, and fuel elements in nuclear reactors [3]. In both cases, it is of paramount importance to understand how vibro-impact systems behave dynamically, and what is the role of the parameter change on the observed dynamical regimes [4,5]. From the purely theoretical point of view vibro-impact oscillators have received a great deal of interest since they are non-smooth dynamical systems for which usual mathematical methods, like bifurcation theory, are applicable only to a limited extent [6–10].

One of the most conspicuous influences on vibro-impact and, in general, on any oscillator system, is caused by extrinsic noise, which is unavoidable in laboratory and industrial contexts. For simple periodic motions the effects of noise are fairly well understood, and their control or suppression can be achieved by standard procedures, like noise

---

* Corresponding author. Tel.: +55 41 3613098; fax: +55 41 3613418.
  E-mail address: viana@fisica.ufpr.br (R.L. Viana).

filtering [11]. Such treatments may fail, however, for complex motions comprising both periodic, quasi-periodic and chaotic regimes, often coexisting with a complicated basin of attraction structure [12]. One of the outstanding features in noisy multistable systems is basin hopping, which consists of the intermittent switching between two or more basins of attraction, when the system is subjected to noise [13–19].

The effects of basin hopping can be dramatically enhanced if the multiple coexisting basins of attraction have fractal boundaries. In this case, it may well happen that even a small amount of noise is able to drive the oscillator out from its asymptotic state to another state, either periodic or chaotic. In vibro-impact systems, in particular, basin hopping can be highly undesirable and even dangerous, since it may produce large amplitude jumps in the oscillations of the moving parts and a consequent fatigue of the material, if not the complete system breakdown. This paper aims to shed some light on the effects of the parametric noise on the dynamics of a prototypical vibro-impact system, specially the intermittent transitions among different asymptotic states due to basin hopping.

This paper is organized as follows: Section 2 presents the prototypical impact-pair system and its equations of motion [20,21]. The noiseless dynamics of this system is considered in Section 3, whereas the effects of parametric noise are dealt with in Section 4. Our conclusions are left to the last section.

2. Mathematical description

In this section we present the basic equations and an impact map of the impact-pair system [20,21]. The impact map is useful to calculate the Lyapunov exponents [22]. The impact-pair system is shown schematically in Fig. 1 and is composed by a point mass m, whose displacement is denoted by x, and an one-dimensional box with a gap of length v. The mass m is free to move inside the gap and the motion of the box is described by a periodic function, $\alpha \sin(\omega t)$.

Equation of motion of the point mass m in the absolute coordinate is

$$\ddot{x} = 0 \tag{1}$$

Denoting the relative displacement of the mass m by y, we have

$$x = y + \alpha \sin(\omega t) \tag{2}$$

Substituting Eq. (2) into Eq. (1), the equation of motion in relative coordinate is

$$\ddot{y} = \alpha \omega^2 \sin(\omega t), \quad -v/2 < y < v/2 \tag{3}$$

Integrating Eq. (3) and invoking initial conditions $y(t_0) = y_0$ and $\dot{y}(t_0) = \dot{y}_0$, the displacement y and the velocity $\dot{y}$, between impacts, are

$$y(t) = y_0 + \alpha \sin(\omega t_o) - \alpha \sin(\omega t) + [\dot{y}_0 + \alpha \omega \cos(\omega t_0)](t - t_0) \tag{4}$$

$$\dot{y}(t) = \dot{y}_0 + \alpha \omega \cos(\omega t_0) - \alpha \omega \cos(\omega t) \tag{5}$$

An impact occurs whenever $y = v/2$ or $-v/2$. After each impact, we apply into Eqs. (4) and (5) the new set of initial conditions (Newton's law of impact)

$$t_0 = t, \quad y_0 = y, \quad \dot{y}_0 = -r\dot{y}, \tag{6}$$

where r is a constant restitution coefficient.

Therefore, the dynamics of the impact-pair system is obtained from Eqs. (4)–(6) and the system depends on control parameters v, r, α, and ω.
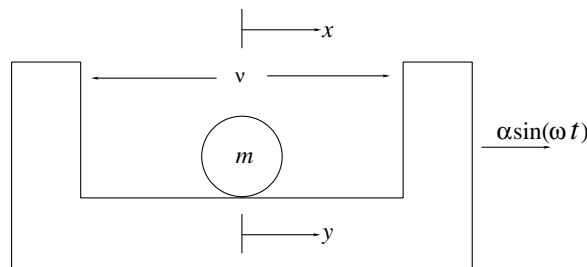

Fig. 1. Model of an impact-pair system.

Since there is an analytical solution for the motion between impacts, we can obtain an impact map, also called transcendental map [22]. First, we define the discrete variables y_n, $\dot{y}_n$, t_n as the displacement, the velocity, and the time (modulo 2π) collected just after the nth impact. Substituting the Newton of impact into Eqs. (4) and (5), we have a two-dimensional map that is given by

$$
\begin{aligned}
y_{n+1} &= y_n + \alpha \sin(\omega t_n) - \alpha \sin(\omega t_{n+1}) + [-r\dot{y}_n + \alpha\omega \cos(\omega t_n)](t_{n+1} - t_n) \\
\dot{y}_{n+1} &= -r\dot{y}_n + \alpha\omega \cos(\omega t_n) - \alpha\omega \cos(\omega t_{n+1})
\end{aligned}
\tag{7}
$$

where $y_n = v/2$ or $-v/2$.

As mentioned before, this map is used in this work to calculate the Lyapunov exponents [22]. Such exponents are computed through $\lambda_i = \lim_{n\to\infty}(1/n)\ln|\Lambda_i(n)|(i=1,2)$, where $\Lambda_i(n)$ are the eigenvalues of the matrix $A = J_1 \cdot J_2,\ldots,J_n$ where J_n is the Jacobian matrix of the map (7), computed at time n.

3. Noiseless dynamics

Initially, we investigate by numerical simulations the dynamical behavior of the impact-pair system (Fig. 1) without noise perturbation in order to determine coexisting attractors. For that, we fix the control parameters at $v = 2.0$ (length of the gap), $\omega = 1.0$ (excitation frequency) and vary the parameters r (restitution coefficient) and α (excitation amplitude).

As a representative example of the kind of dynamics generated by the impact-pair system, we present in Fig. 2(a) a bifurcation diagram for the velocity, $\dot{y}_T$, versus the amplitude excitation, α. The dynamical variable $\dot{y}_T$ is obtained from a stroboscopic map (Time-2π). In the diagram, we can see two-coexisting attractors (plotted in gray and in black) for some range of the control parameter; for example, there are two period-1 orbits at $\alpha = 3.25$. In this case, these attractors are symmetric and appear due to the pitchfork bifurcation at $\alpha \approx 3.0228$.

In order to characterize the nature of the behavior observed in Fig. 2(a), we show in Fig. 2(b) the Lyapunov exponents for the attractors plotted in black. If the largest Lyapunov exponent is positive the attractor is chaotic, if not the attractor is periodic. As mentioned before, to calculate the Lyapunov exponents we use the impact map according the algorithm presented in Ref. [22] and shortly described in Section 2.

To better analyze the dynamics of the coexisting attractors at $\alpha = 3.25$, we depict in Fig. 3(a) another bifurcation diagram of the two-coexisting attractors in terms of the restitution coefficient, r. This diagram shows that the evolution of these attractors is given by a reverse period-doubling bifurcation cascade. Fig. 3(b) shows the Lyapunov exponents corresponding to the attractors of the Fig. 3(a) plotted in black.
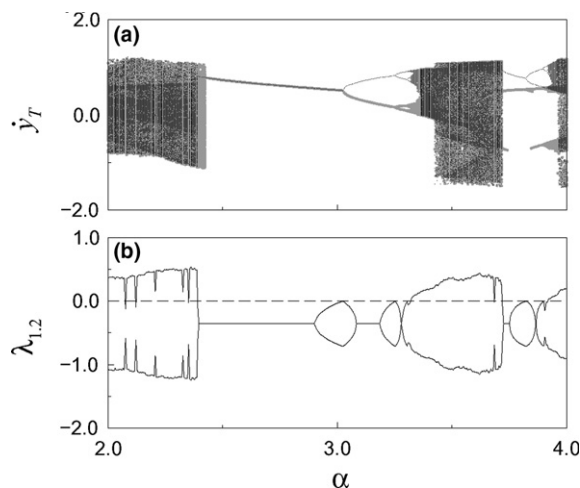

Fig. 2. (a) Bifurcation diagram showing two-coexisting attractors (gray filled circles and black points) for the velocity $\dot{y}_T$, for a stroboscopic map, as a function of the amplitude excitation, α and (b) the Lyapunov exponents, $\lambda_{1,2}$, for the attractor plotted in black. For the control parameter $r = 0.7$.
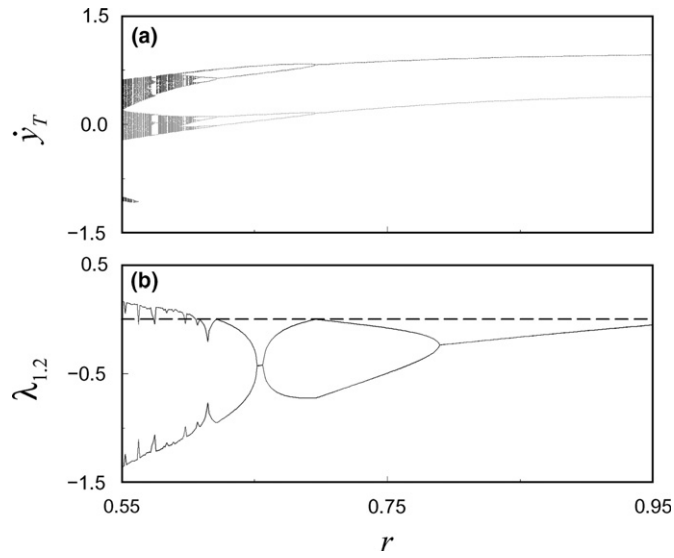
Fig. 3. (a) Bifurcation diagram showing two-coexisting attractors (gray and black) for the velocity $\dot{y}_T$, for a stroboscopic map, as a function of the coefficient of restitution, r and (b) the Lyapunov exponents for the attractors plotted in black, for the control parameter $\alpha = 3.25$.
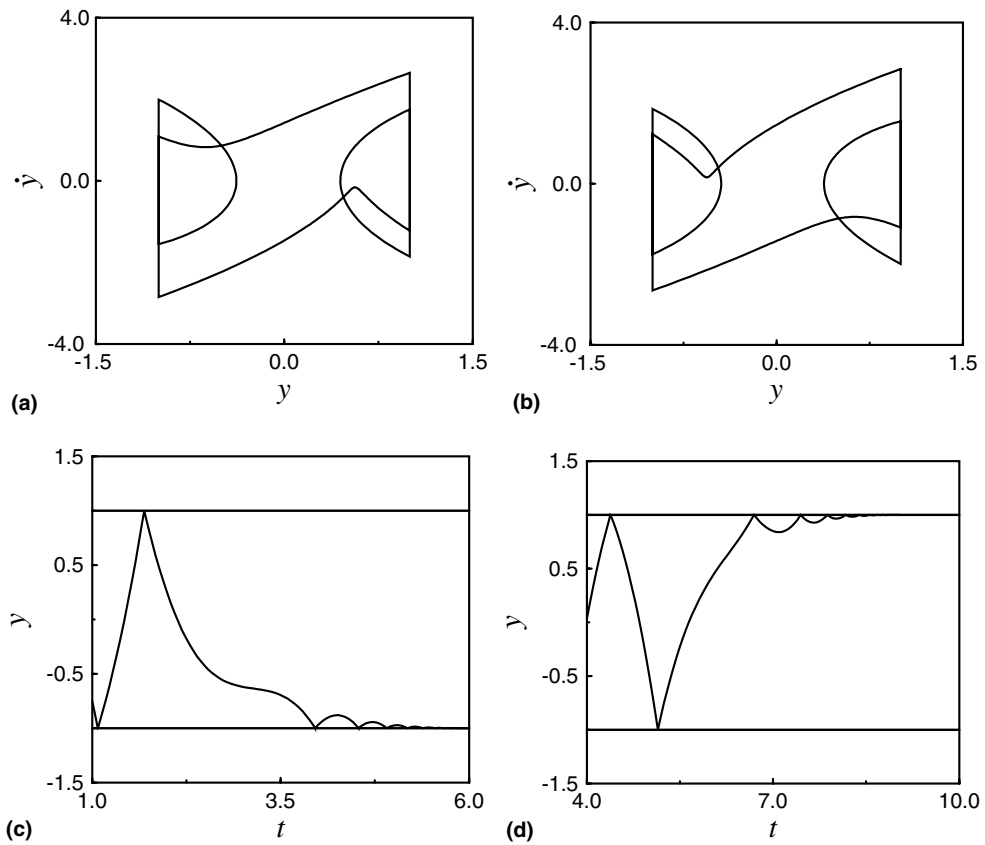

Fig. 4. Phase portrait of velocity versus displacement of two coexisting periodic attractors (a) and (b), that can be seen in Figs. 2(a) and 3(a); time histories of two equilibrium points (c) and (d), for the control parameters $\alpha = 3.25$ and $r = 0.7$.
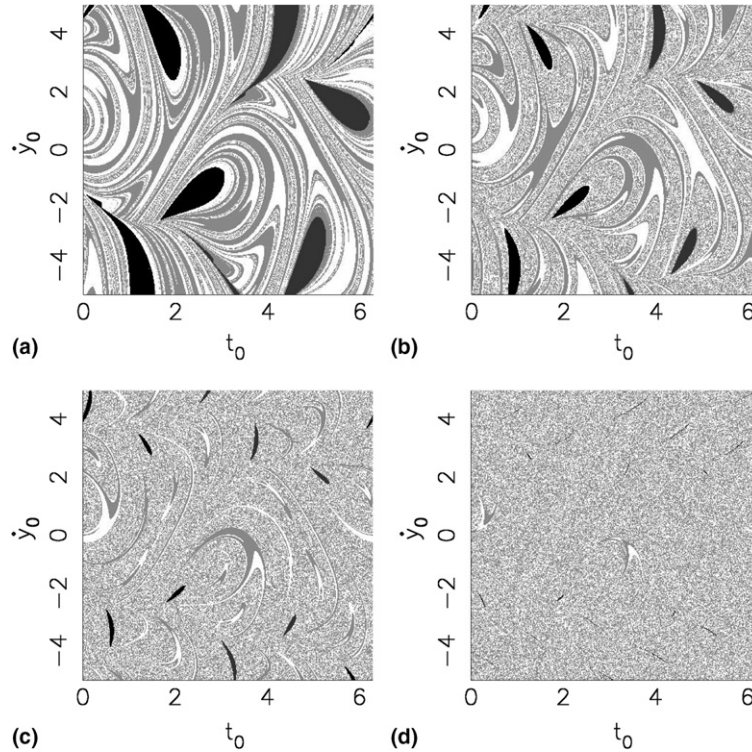
Fig. 5. Basins of attraction, in white and light gray, for the two coexisting attractors shown in Fig. 3(a) and, in dark gray and black, two equilibrium points (shown in Fig. 4(c) and (d)), for the restitution coefficient fixed at $r = 0.6$ (a), $r = 0.7$ (b), $r = 0.8$ (c), and $r = 0.9$ (d), for the control parameter $\alpha = 3.25$.

Phase portraits of the two symmetrical coexisting periodic attractors, for $\alpha = 3.25$ and $r = 0.7$, are shown in Fig. 4(a) and (b). Besides these attractors, for the same set of parameters we identify two equilibrium points that are shown in Fig. 4(c) and (d). In Fig. 5(b) we present the basins of these attractors.

To evaluate the basins structure for the attractors (shown in Fig. 3(a)) and the two equilibrium points (Fig. 4(c) and (d)), we fix a value $y_0 = 0$ and work with a two-dimensional section of the phase space $(\dot{y}_0, t_0)$. For a grid of 400×400 pixels, we present the evolution of the basins structures in Fig. 5(a) and (b). First, in Fig. 5(a) we see the basins of the chaotic attractors, plotted in white and light gray, and of the equilibrium points, in black and dark gray. As can be seen the basin boundary between chaotic attractors is apparently fractal, whereas the basin of the equilibrium points is smooth.

4. Noise dynamics

In this section, we investigate the effects of a parametric noise perturbation on the performance of the impact-pair system. For that, we consider a random perturbation on the control parameter α. In other words, it is considered a parametric noise in following form:

$$\alpha \rightarrow \alpha(1 + \sigma p_n) \tag{8}$$

where p_n represents a uniform random variable on the interval $(-1, +1)$ with unit variance and zero mean, and σ is referred to as the noise level of the parametric fluctuations. In addition, the σp_n term is applied just after the moment of the impact.

Let us study the effects of such noise in the dynamical scenario of the impact-pair system. As an example, we consider the case of the coexisting periodic attractors shown in Fig. 4(a) and (b). First, adding a small amount of noise, 0.8%, we do not observe noticeable dynamical effects; see Fig. 6(a). Increasing the noise levels, in Fig. 6(b) and (c), we see the attractor hopping phenomena. In other words, the trajectory visits alternately, by sudden bursts, the two
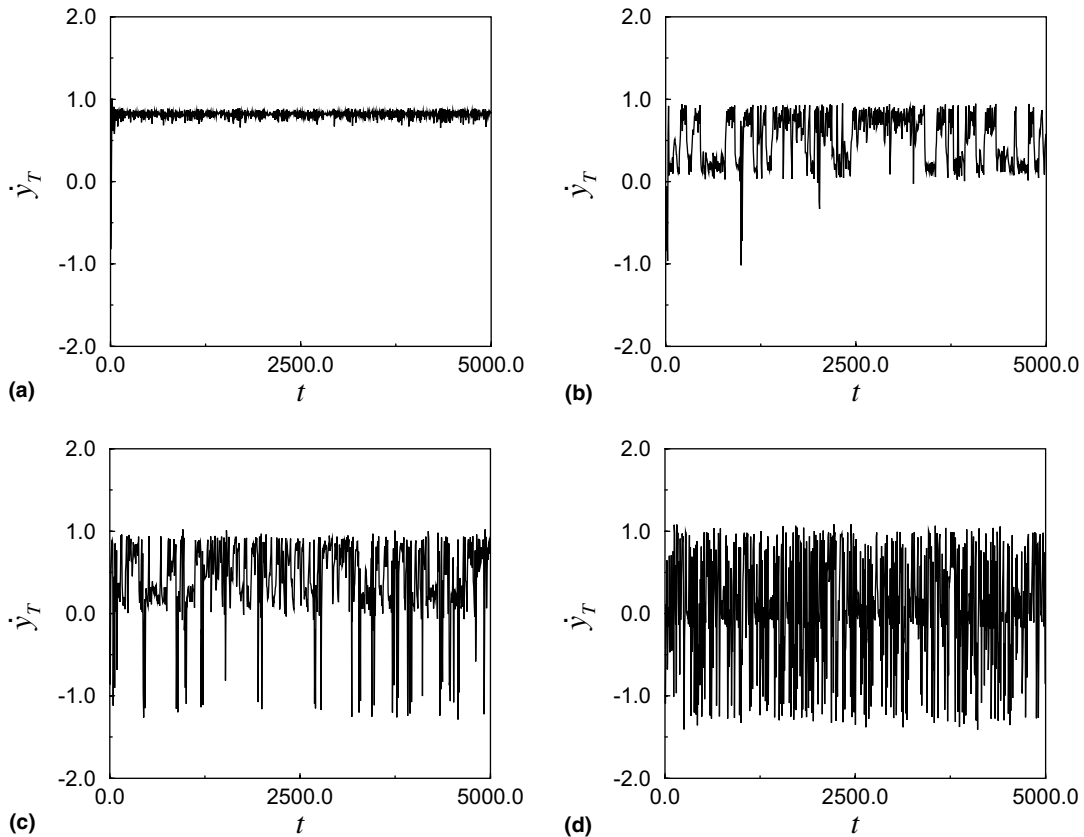
Fig. 6. Time series for the stroboscopic velocity $\dot{y}_T$, for $\alpha = 3.25$ and $r = 0.7$, and increasing noise: (a) $\sigma = 0.008$; (b) $\sigma = 0.03$, (c) $\sigma = 0.1$ and (d) time series of a chaotic attractor for $\alpha = 3.5$ and $r = 0.7$.

coexisting attractors. Moreover, we can also observe during the bursts that the trajectory leaves the neighborhood of the attractors and spend a certain time in the chaotic saddle. To clarify the last statement, we show in Fig. 6(d) the time series of a chaotic attractor and we can see here the same pattern of the evolution. In addition, we depict in Fig. 7(a) and (b) the orbit of this chaotic attractor (in black) and the orbit for the system with 5% of noise perturbation (in gray). As can be seen the orbit with noise and the chaotic attractor occupy practically the same place in the space phase. The corresponding Lyapunov exponents are plotted in Fig. 7(c).

Now we determine how much noise level is necessary to observe basin hopping. For this purpose, we construct a diagram in the control parameter space, as shown in Fig. 8, using practically the same range of the restitution coefficient parameter of the bifurcation diagram (Fig. 3(a)). The white region shows values of noise where we observe basin hopping. From this result, considering that low level of noise implies in basin hopping phenomena, we can say that noise has an important role in the dynamical behavior of the impact-pair system.

Even a superficial inspection of Fig. 6(b) and (c) already shows us that the intermittenty switchings between coexisting dynamical states occur at different time intervals τ. In this case, it is useful to compute the (normalized) probability distribution function (PDF) for these values, $P(\tau)$, such that $P(\tau)d\tau$ is the number of switching intervals with durations between τ and $\tau + d\tau$. For the system parameters chosen in Fig. 6(a)–(c), this distribution turns to be an exponential function of τ for distinct values of the noise level (Fig. 9):

$$P(\tau) = \frac{1}{\mu} \exp\left(-\frac{\tau}{\mu}\right) \tag{9}$$

where the effect of increasing noise levels is to increase the slope $1/\mu$ of the distribution. This is easily explained by considering that as much noise there is in the system, more frequent are basin jumps, so that most of the switching intervals are very short. In this case, the average switching time is
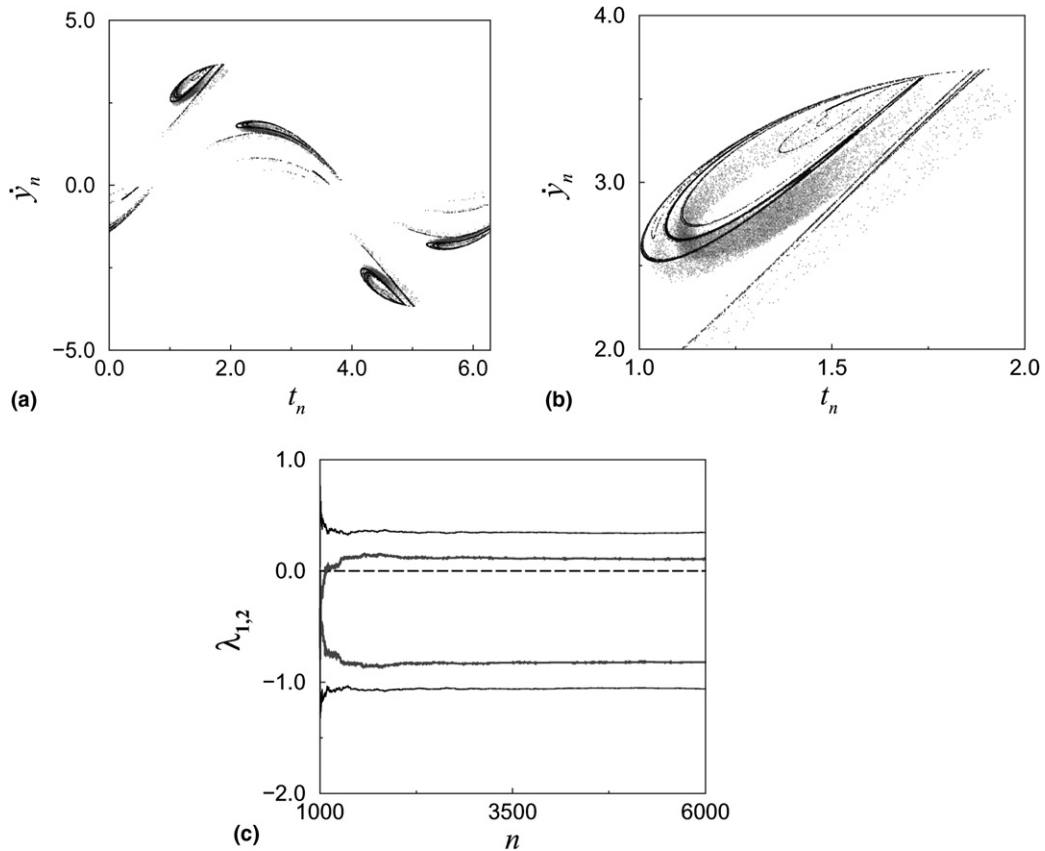
Fig. 7. For the coefficient of restitution fixed at $r = 0.7$. (a) Poincaré map $(\dot{y}_n, t_n)$ just before the impact at $y = |v/2| = 1.0$. In black a chaotic attractor for $\alpha = 3.5$, see Fig. 2(a). In gray attractors hopping for $\alpha = 3.25$ and the noise level $\sigma = 0.05$, (b) magnification of a portion of the previous figure, (c) the convergent series of the Lyapunov exponents, $\lambda_{1,2}$, as function of the impact number, n, for the orbits of (a); black for the chaotic attractor and gray for the attractors hopping.
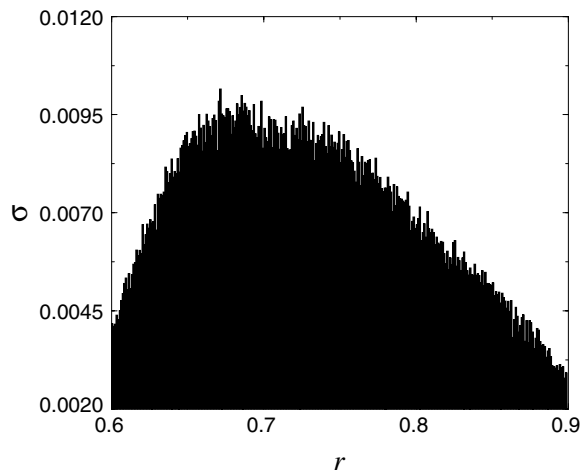

Fig. 8. Noise level, σ, as a function of the restitution coefficient, r. The white region indicates for which values of noise the basin hopping is observed.
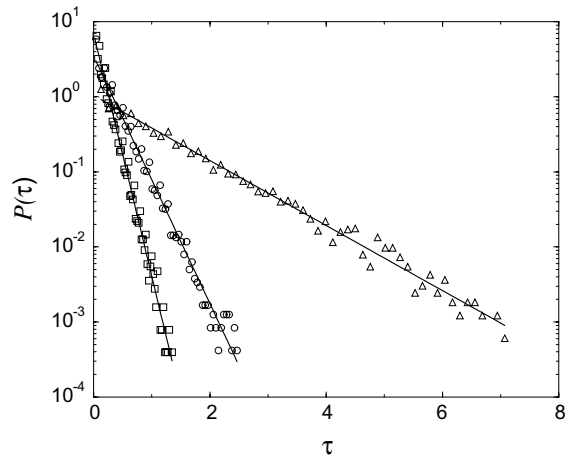
Fig. 9. PDF for different noise level. Solid lines associated to symbols correspond to the fitting. ($\triangle$) $\sigma = 0.02$, slope $= -0.997$, ($\bigcirc$) $\sigma = 0.03$, slope $= -3.797$ and ($\square$) $\sigma = 0.04$, slope $= -7.445$.

$$\langle \tau \rangle = \int_0^\infty P(\tau) \tau \, \mathrm{d}\tau = \mu \tag{10}$$

On that basis, one can also expect that the average switching time, which we can numerically approximate to the temporal mean

$$\langle \tau \rangle = \frac{1}{N_s} \sum_{i=1}^{N_s} \tau_i \tag{11}$$

where N_s is the number of switching intervals during the considered time period, would decrease if we increase the noise level σ. Fig. 10 shows that this is actually the case. Our numerical results are fitted by the following equation:

$$\langle \tau \rangle = c\sigma^b \exp(2a \ln \sigma) \tag{12}$$

which shows, for low noise levels, a power-law scaling, with an exponential tail for high noise.

In addition, we show that the basins structure of the equilibrium points, shown in Fig. 4(c) and (d), practically does not change as a function of the noise level. For that, we pick up a box from Fig. 5(b) focusing on this basin structure
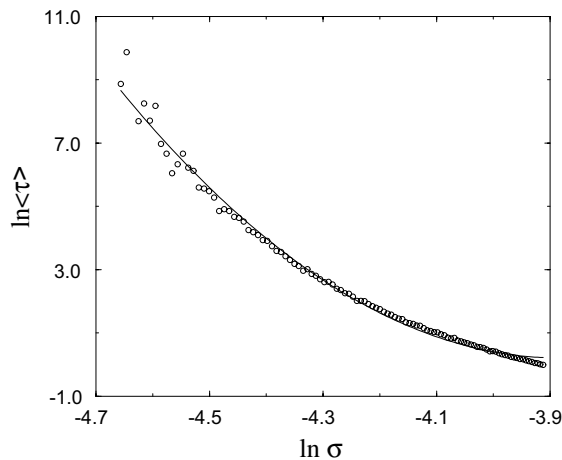

Fig. 10. Time averaged in a basin as a function of the noise level. $\langle \tau \rangle = c\sigma^b \exp[a(\ln \sigma)^2]$, where $a = 14.09$, $b = 109.40$, and $c = \exp(212.5)$.
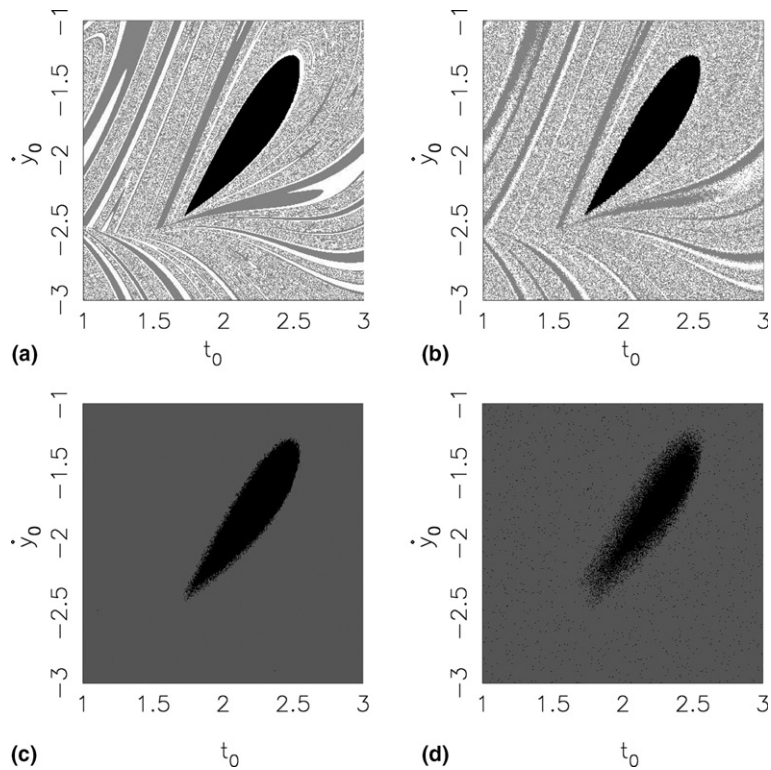
Fig. 11. Magnification of the Fig. 5(b) without noise perturbation (a) and basins of the attraction for the noise levels $\sigma = 0.008$ (b), $\sigma = 0.03$ (c), and $\sigma = 0.10$ (d). In dark gray it is plotted the basin of the attractors hopping.

plotted in black. As first step, we use a tiny amount of noise, 0.8%. The result is shown in Fig. 11(b) where we can just note a slight change on the basins of the two periodic attractors plotted in white and light gray. Even for higher noise level, we verify the robustness of this structure as shown in Fig. 11(c) and (d) for the noise perturbation 3% and 10%, respectively.

5. Conclusion

Although vibro-impact systems of engineering interest may present a wide variety of forms, ranging from impact hammers to shock absorbers, we can grasp the essentials of their dynamics from analyzing simpler models. In this paper we pursued this task by considering the one-dimensional motion of a cart, externally driven by a sinusoidal source, and containing a sphere undergoing inelastic collisions with its walls. The noiseless dynamics is found to exhibit, for some range of the system parameters, coexistence of attractors with a complicated boundary. The addition of parametric noise causes basin hopping, or the alternate switching among different coexisting attractors. These alternations occur between different time intervals obeying an exponential distribution. The average duration of such intervals decreases with increasing noise level, and satisfies a scaling law. We were able to describe some parameter ranges for which basin hopping is observed, in terms of the parametric noise level.

The theoretical explanation of basin hopping is based in the properties of the chaotic saddles which lie in between the basins. The noise term kicks the trajectory out of an open neighborhood of some attractor into the basin boundary. The trajectory spends there a certain amount of time until it reaches again the neighborhood of the same or another attractor. The chaotic saddle underlying the basin boundary structure is a non-attracting chaotic invariant set, so that the trajectory, while wandering in the vicinity of the saddle, experiences a transient chaotic motion. This chaotic transient is related to the chaotic saddle existing in between the coexisting basins and, in presence of noise, can be sustained to yield an apparently stationary regime very similar to a noiseless chaotic attractor.

Acknowledgements

References

[1] Blazejczyk-Okolewska B, Czolczynsky K, Kapitaniak T, Wojewoda J. Chaotic mechanics in systems with friction and impacts. Singapore: World Scientific; 1999.

[2] Blazejczyk-Okolewska B, Czolczynsky K, Kapitaniak T. Classification principles of types of mechanical systems with impacts—fundamental assumptions and rules. Eur J Mech—A/Solids 2004;23(3):517–37.

[3] Jerrelind J, Stensson A. Nonlinear dynamics of parts in engineering systems. Chaos, Solitons & Fractals 2000;11:2413–28.

[4] Kapitaniak T. Chaos for engineers. New York, Berlin, Heidelberg: Springer; 2000.

[5] Wiercigroch M, de Kraker B. Applied nonlinear dynamics and chaos of mechanical systems with discontinuities. Singapore: World Scientific; 2000.

[6] Thompson JMT. Global dynamics of oscillations: fractal basins and intermediate bifurcations. In: Aston PJ, editor. Nonlinear mathematics and its applications. Cambridge: Cambridge University Press; 1996.

[7] Nordmark AB. Non-periodic motion caused by grazing incidence in an impact oscillator. J Sound Vibr 1991;145:279–97.

[8] Dankowicz H, Piiroinen P, Nordmark AB. Low-velocity impacts of quasi-periodic oscillations. Chaos, Solitons & Fractals 2002;14:241–55.

[9] Pavlovskaia E, Wiercigroch M. Analytical drift reconstruction for visco-elastic impact oscillators operating in periodic and chaotic regimes. Chaos, Solitons & Fractals 2004;19:151–61.

[10] de Souza SLT, Caldas IL, Viana RL, Balthazar JM. Sudden changes in chaotic attractors and transient basins in a model for rattling in gearboxes. Chaos, Solitons & Fractals 2004;21:763–72.

[11] Davenport Jr WB, Root WL. An introduction to the theory of random signals and noise. New York, NY, USA: McGraw-Hill Inc.; 1958.

[12] Kapitaniak T. Chaos in systems with noise. Singapore: World Scientific; 1988.

[13] Kraut S, Feudel U, Grebogi C. Preferences of attractors in noisy multistable systems. Phys Rev E 1999;59:5253–60.

[14] Kraut S, Feudel U. Multistability, noise, and attractor hopping: the crucial role of chaotic saddles. Phys Rev E 2002;66:015207(R).

[15] de Souza SLT, Caldas IL, Viana RL, Batista AM, Kapitaniak T. Noise-induced basin hopping in a gearbox model. Chaos, Solitons & Fractals 2005;26:1523–31.

[16] Rajasekar S, Valsakumar MC, Paul Raj S. Noise-induced jumps in two coupled duffing oscillators. Physica A 1998;261:417–34.

[17] Gan C. Noise-induced chaos and basin erosion in softening duffing oscillator. Chaos, Solitons & Fractals 2005;26:1069–81.

[18] Liu Z, Ma W. Noise induced destruction of zero Lyapunov exponent in coupled chaotic systems. Phys Lett A 2005;343:300–5.

[19] Patnaik PR. Application of the Lyapunov exponent to detect noise-induced chaos in oscillating microbial cultures. Chaos, Solitons & Fractals 2005;26:759–65.

[20] Han RPS, Luo ACJ, Deng W. Chaotic motion of a horizontal impact pair. J Sound Vibr 1995;181:231–50.

[21] Luo ACJ. Period-doubling induced chaotic motion in the LR model of a horizontal impact oscillator. Chaos, Solitons & Fractals 2004;19:823–39.

[22] de Souza SLT, Caldas IL. Calculation of Lyapunov exponents in systems with impacts. Chaos, Solitons & Fractals 2004;19:569–79.